JOURNAL OF MATERIALS SCIENCE 15 (1980) 1–19

Review

Principles of photoelectrochemical solar energy conversion

M. A. BUTLER, D. S. GINLEY
Sandia Laboratories, US Department of Energy, Albuquerque, New Mexico 87185, USA

Photoelectrochemical devices for conversion of solar energy into both electrical energy and chemical energy are discussed with emphasis on how the various material properties of the photoactive electrodes influence device efficiency and stability. The similarity between photoelectrochemical cells (PECs) and solid state devices is used to model their behaviour and optimize such parameters as band gap, doping level, minority carrier lifetime, etc. A model is presented which calculates the electron affinity of any semiconductor and allows the prediction of the open circuit voltage of wet photovoltaic cells and optimum biasing for chemical producing cells. The effects of absorbed ions at the semiconductor/electrolyte interface are reviewed. The temperature dependence of the energy levels in the semiconductor and the electrolyte are considered and the implications of these results to operation of PECs at elevated temperature are discussed. The major differences between PECs and solid state devices are the stability considerations. The thermodynamics of this problem is discussed. Other important degradation mechanisms and some solutions to these problems are reviewed. Finally, a prognosis of the future of this field is presented.

1. Introduction

The energy crisis of the seventies has stimulated research in energy related areas, particularly those useful for utilization of solar energy. One of the many research fields which show promise for solar energy conversion is photoelectrochemistry. A photoelectrochemical device is one in which a semiconducting electrode is illuminated in a liquid cell and drives electrochemical reactions at both electrodes. These cells may be of two types; one directed primarily at the production of electricity (wet photovoltaic cell) and one making chemical products through a chemical change in the electrode or electrolyte. One of the more attractive chemical reactions is the decomposition of water to form H_2 and O_2 (photoelectrolysis).

An important aspect of the problem of applying photoelectrochemical devices to solar energy conversion is defining the materials properties of the light-sensitive electrode necessary to optimize its performance. Summarizing the progress in this area is the goal of this review. In order to do this, we must delve into the details of the mechanisms involved in the photoelectrochemical process. As you will see, the field has progressed to the point of being able to define the desirable features of a photoelectrode, but has not yet completely solved the problem of finding such a material.

Photoeffects at electrodes in electrochemical cells were first observed by Becquerel [1] in 1839. Since that time there has been sporadic interest in this field, dictated more by interest in related fields than by interest in semiconductor photoelectrochemistry itself. Thus, historically it was an interest in understanding semiconducting properties for solid state devices which resulted in advances in semiconductor photoelectrochemistry [2]. In the last two decades interest in semiconductor photoelectrochemistry itself has blossomed due in no small part to the pioneering work of Gerischer [3, 4].

Application of this knowledge to energy conversion was first shown by Fujishima *et al.* in 1969 [5], who demonstrated the photodecomposition of

0022–2461/80/010001–20$04.00/0

water at a TiO_2 electrode. This information and their subsequent work [6] made little impression until the energy crisis of the early seventies. By 1975, there were a number of groups around the world working on this problem and the number of papers in the field was growing almost exponentially.

A number of review articles have been written in this field and we refer the reader to these for a more general review of the subject [7–9]. A particularly complete review is that by Nozik [10]. In this review, we will concentrate on the optimum material properties of the light-sensitive electrode of a photoelectrochemical cell (PEC).

The easiest way to describe the operation of a photoelectrochemical cell is to examine its energy level diagram. The simplest device consists of a semiconducting electrode, a metallic electrode and a "simple" electrolyte as shown in Fig. 1.

The energy in the electrolyte at which electrons must be provided to drive the electrochemical reaction is known as the redox potential and is usually referenced to the normal hydrogen or saturated calomel electrodes, NHE and SCE, respectively. The energy position at which the conduction and valence bands for n- and p-type semiconductors respectively intercept the solid electrolyte interface is known as the flatband potential V_{fb}. This is because V_{fb} is determined from the changing properties of the interface (capacitance, photocurrent, etc.) as the bands are made flat.

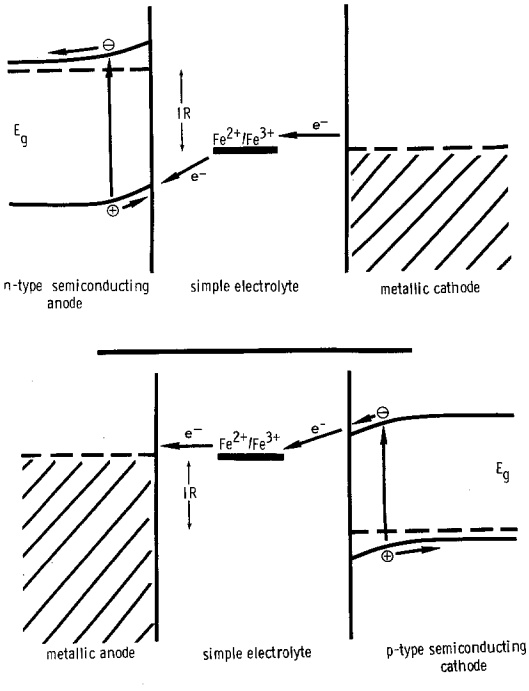

Figure 1 Energy level diagram for simple electrochemical devices which produce electricity but no chemical products. The use of both n- and p-type semiconducting electrodes is illustrated. A simple electrolyte is one in which only a single electrochemical reaction can take place.

The semiconductor can be used as a light-sensitive anode or cathode depending on whether it is n- or p-type, respectively. This is determined by the need for a region depleted of majority carriers at the semiconductor surface. In the depletion region there exists an electric field which is necessary to separate spatially the optically excited electron in the conduction band from the hole in the valence band. Thus, when illuminated with photons of energy greater than the band gap of the semiconductor, an electron is excited into the conduction band and the electron and hole are separated by the electric field in the depletion region before they can recombine. The majority carrier then flows through the electrical load to the metallic electrode and drives an electrochemical reaction. The minority carriers flow to the semiconductor surface driving another electrochemical reaction.

In a "simple" electrolyte only one electrochemical reaction is possible. This is clearly not a realistic situation since all electrolytes have several possible electrochemical reactions. But, it does allow us to describe the operation of these devices in the simplest manner. Fig. 1 represents the single electrochemical reaction by the reversible ferric–ferrous couple ($Fe^{3+}_{aq} + e^- \leftrightarrows Fe^{2+}_{aq}$). In such an electrolyte the reaction is driven one way at the anode ($Fe^{2+}_{aq} \rightarrow Fe^{3+}_{aq} + e^-$) and the opposite direction at the cathode ($Fe^{3+}_{aq} + e^- \rightarrow Fe^{2+}_{aq}$). Thus, in such a system there is no net chemical change and the power produced must be extracted via the electrical load. Such cells are commonly called wet photovoltaic cells in analogy with the corresponding solid state devices.

Another type of PEC results in the production of a chemical product. Its energy level diagram is illustrated in Fig. 2. The operation of the device is the same as that just discussed, except that two irreversible electrochemical couples are driven, with one taking place at the anode and the other at the cathode. This results in a net chemical change in the electrolyte. In the figure we illustrate this by the reactions for the decomposition of water to hydrogen and oxygen. At the cathode, the reaction is ($2H^+ + 2e^- \rightarrow H_2$) and at the anode the reaction is ($2OH^- \rightarrow 2H^+ + O_2 + 4e^-$). This reaction is photosynthetic in that external energy

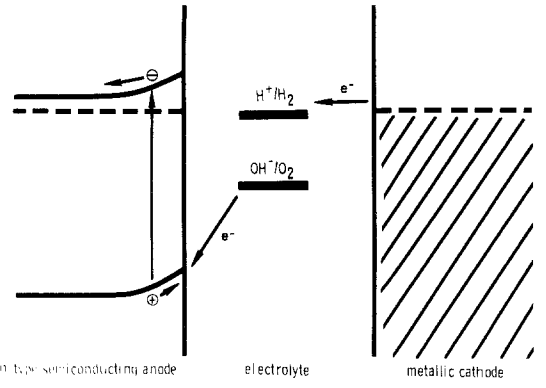

Figure 2 Energy level diagram for an electrochemical device which produces a chemical product. The electrolyte is illustrated for the decomposition of water into H_2 and O_2. Only an n-type semiconductor is shown, although a p-type semiconductor could be used as illustrated in Fig. 1. Normally, chemical producing cells are operated under short-circuit conditions to maximize the amount of the chemical product.

must be provided to derive this reaction*. Note that the net amount of energy stored is the difference between the redox potentials of the two couples. There are also photocatalytic reactions which are thermodynamically favourable but would have very slow kinetics without the participation of the photoexcited semiconducting electrode.

It must be stressed that decompositon of water is not the only possible method of turning solar energy into chemical energy. Many other interesting reactions exist and need exploring. For example, it may be possible by this method to generate NH_3, a fertilizer, from H_2O and N_2 [12].

These, then, are the two basic types of photoelectrochemical devices. An important variation on the PECs described is the dye-sensitized cell illustrated in Fig. 3. In this case, the optical properties of the cell are determined by the dye adsorbed or chemisorbed on the semiconductor surface. Once the excited electron from the dye has been injected into the semiconducting electrode, the behaviour and important characteristics of the cell are similar to other PECs.

Other forms of cell can, of course, be made which combine the basic ideas presented here. For example, both photosensitive anodes and cathodes can be used or a cell can be operated so as to produce both electricity and a chemical product. However, an appreciation of these systems only requires an understanding of the basic photoelectrochemistry at a single semiconductor/electrolyte interface. Thus, we shall concentrate on this aspect of the problem.

From examining these energy level diagrams, it is possible to discern the basic criteria that a useful semiconducting electrode must satisfy. The first important aspect is efficient conversion of photons to excited electrons and their efficient utilization in the electrochemical processes. In general, in these cells the generation and separation of carriers in the semiconductor is the rate limiting step rather than the chemical kinetics at the interface. Thus, the problem becomes the same basic problem as is faced in solid-state photovoltaic devices and the same factors are important. Since only photons of energy larger than the band gap of the semiconductor can be used, the band gap must be chosen to optimize the conversion efficiency. Another factor is the optical absorption depth compared to the depletion layer thickness. Since we need the electric field in the depletion layer to separate the electron–hole pairs and since most charge carriers in semiconductors have short dif-

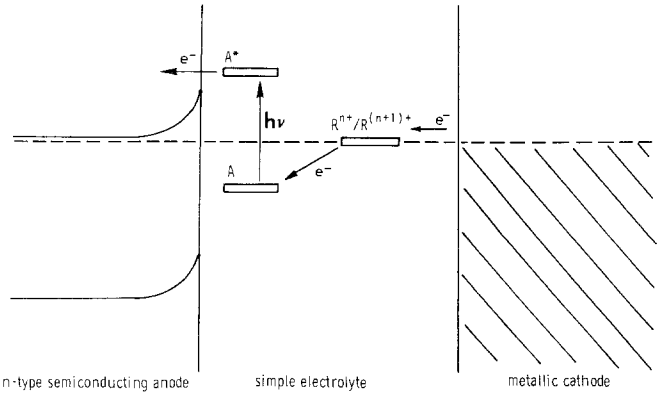

Figure 3 Energy level diagram for a dye-sensitized photoelectrochemical cell. The absorption of a photon by the dye A chemisorbed at the semiconductor surface raises the energy of an electron in the dye to A^* its excited state, energetic enough for the electron to be injected into the semiconductor. The ionized dye molecule is then returned to its ground state by obtaining an electron from the redox couple in the electrolyte. The rest of the behaviour of the cell corresponds to other photoelectrochemical cells.

* The distinction of photosynthetic and photocatalytic was pointed out by Bard [11].

fusion lengths, it is important to absorb most of the light in the depletion layer region. The optical absorption depth will be significantly different if the gap is direct rather than indirect. The depletion layer thickness depends on doping level and dielectric constant of the semiconductor. Clearly, some model is necessary to optimize the numerous parameters and this will be addressed in detail in the next section.

The second important property of the semiconducting electrode is the location of the energy bands. Aside from determining the band gap, the energy band positions relative to the energy levels in the electrolyte also determine the maximum open-circuit voltage for the wet photovoltaic cells and the biasing requirements, if any, for the chemical producing cells. This can be seen by examining Figs. 1 and 2. For the wet photovoltaic cells shown in Fig. 1, under open-circuit conditions the Fermi level in the metal electrode will equal the redox potential in the electrolyte. Under maximum illumination, the bands in the semiconductor will approach flatband condition. Thus, the maximum open-circuit voltage for the cell will be the difference between the redox potential in the electrolyte and the intercept of the conduction band with the interface (the electron affinity of the semiconductor). While the redox potential is known for most couples the same cannot be said of semiconductor electron affinities. This means that either this information must be determined experimentally in each case or a model to predict semiconductor electron affinities must be constructed. In Section 3, a model is reviewed which allows the simple calculation of the electron affinity of any compound.

Similar arguments apply to the chemical producing cell shown in Fig. 2. Since it would be desirable to operate the cell under short-circuit conditions and maximize the production of chemical products, the conduction band must intercept the interface so that a depletion region exists at short circuit conditions. Thus for an n-type semiconductor the electron affinity must be smaller than the cathodic redox potential in the electrolyte as measured from the vacuum level. Conversely, for a p-type semiconductor the valence band should intercept the interface below the anodic redox potential in the electrolyte.

As in any interdisciplinary field, confusion with regard to nomenclature can often arise. Electrochemists traditionally measure redox potentials from the normal hydrogen electrode (NHE) and physicists measure electron energies from the vacuum level. To convert from the electrochemists scale to physicists scale, add 4.5 eV [13].

The third and perhaps most crucial condition that the semiconducting electrodes must satisfy is stability under the rather rigorous conditions in which they are operated. They must not only be stable against chemical dissolution in the electrolyte but also stable against electrochemical corrosion and photocorrosion. Most of these effects are not well understood so that choosing stable materials or modifying their properties or the electrolyte to induce stability is more art than science. Some progress has recently been made in defining the conditions for stability of semiconductors in contact with electrolytes [14, 15]. The decomposition reactions are merely additional redox couples in the electrolyte. Thus, the relative positions of these couples with respect to the semiconductor band edges will determine the thermodynamic stability of the semiconductor in that particular electrolyte. However, some semiconductors which are thermodynamically unstable may appear stable if the kinetics of the decomposition reaction are slow enough. There is also the problem of competition between the decomposition reaction and other possible reactions both beneficial and detrimental. Stability is a complex question which is quite difficult to answer even on an individual basis.

These three criteria: (1) quantum efficiency, (2) potential behaviour, and (3) stability, define the characteristics desirable in a semiconducting photoelectrode. In the next three sections, each of these criteria will be considered individually and in detail.

2. Quantum efficiency

Fig. 1, shows that the photoresponse of a semiconducting electrode is a two-step process. A minority carrier is first generated in the semiconductor by the absorption of a photon and transported to the semiconductor/electrolyte interface. This step is completely controlled by the properties of the semiconductor. The second step is the electrochemical reaction at the semiconductor surface which transfers charge through the interface. This step depends on the properties of both the electrolyte and the semiconductor. For all semiconducting electrodes, one of these two steps will be rate determining. If the first step is the rate

limiting step, then the electrochemical kinetics play no role and the semiconductor/electrolyte junction can be treated exactly as a solid-state Schottky junction. With the second step the rate limiting step, the behaviour of the junction is much more complex. The dominant behaviour may be determined by examining the photocurrent as a function of incident light intensity.

Fig. 4 shows such a plot for WO_3 [16]. The linear behaviour observed would be expected when the carrier generation is the rate-limiting step. Limitation by the electrochemical kinetics would result in saturation of the photocurrent at higher light intensities. Our observations indicate that, at least in the metal oxide semiconductors, the carrier generation process is always rate-limiting. This result is supported by measurements at a light flux as high as 380 W cm^{-2} using laser illumination [17]. The same observation appears to hold for a large number of the non-oxides employed in wet photovoltaic cells but only in the limited regime of fairly low-light intensities. Below about two suns, carrier generation appears rate-limiting in most of the viable systems.

The lack of importance of electrochemical kinetics is rather surprising. Reaction kinetics are generally described using the Butler–Volmer equation [18]:

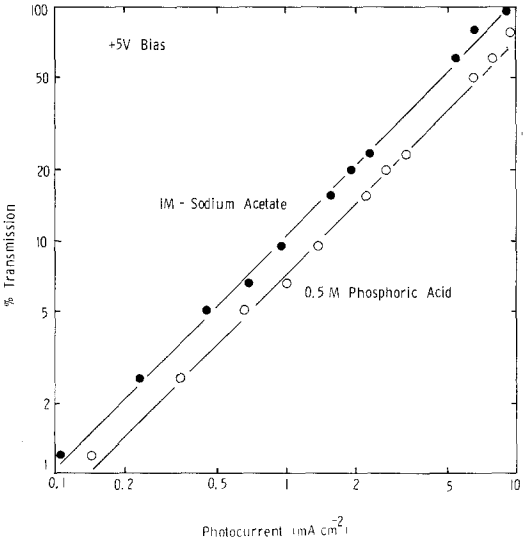

Figure 4 Photocurrent versus light intensity for a WO_3 electrode biased to + 5 V in the different electrolytes. 100% transmission corresponds to a photon flux of 10 suns (1 W cm^{-2}) from a focused Xenon lamp. The per cent transmission is varied by the use of neutral density filters.

$$i = i_0\{\exp[(1-\beta)qU/k_BT] - \exp[-\beta qU/k_BT]\}, \quad (1)$$

where i_0 is the exchange current density, U the overpotential required to drive a current i through the electrode, q is the charge transferred per ion, k_B Boltzmann's constant, T the absolute temperature and β is a parameter involving the nature of the reaction (usually $\beta \approx \frac{1}{2}$). Since negligible potential is required for $i \ll i_0$, the overpotential required depends strongly on the size of i_0. For oxygen evolution on platinum (one of the better metal electrodes for this reaction) we have $i_0 \sim 10^{-9}$ A cm^{-2} [19]. Since current densities are observed on WO_3 of 10^{-2} A cm^{-2} and larger, this implies that a large built-in overpotential must exist in order that the kinetics are not the rate-limiting step.

The origin of this overpotential can be seen by looking at Fig. 2. Since the oxygen evolution reaction involves transfer of an electron from the redox potential to the top of the semiconductor's valence band, this reaction is driven by the potential $U = E_g - 1.23\text{ eV} - V_{bb}$ where E_g is the band gap of the semiconductor, 1.23 eV the potential to decompose water and V_{bb} the band bending under short-circuit conditions. This potential is independent of applied potential since the hydrogen redox potential and semiconductor electron affinity are independent of the applied potential. This picture of the overpotential at semiconductor electrodes has been used to estimate the minimum bandgap required for efficient solar energy conversion [20].

When the electrochemical kinetics can be ignored, a photoelectrochemical cell can be treated very much as a solid-state solar cell. The most important factor determining the efficiency of the device is then the match of the semiconductor band gap to the solar spectrum. The solar spectrum is shown in Fig. 5.

There are two competing factors which determine the optimum band gap E_g. Since only photons of energy greater than E_g will contribute to the photocurrent, E_g must be as small as possible. However, every photon absorbed by the semiconductor, irrespective of its energy, can contribute at most the energy E_g. Thus, to maximize the energy conversion efficiency per photon it is necessary to maximize the band gap. From this we would expect that the maximum power the solar cell is capable of producing

would be:

$$P = E_g \int_{E_g}^{\infty} N(E)\,dE, \qquad (2)$$

where $N(E)$ is the number of photons cm^{-2} sec^{-1} eV^{-1} as shown in Fig. 5. This maximum power level is never achieved due to other loss mechanisms. For a detailed discussion see Hovel [22]. These arguments suggest an optimum bandgap at around 1.5 eV. The necessity of having sufficient overpotential to overcome the electrochemical kinetics as discussed in [19] adds several tenths of an eV to the estimate and suggests the optimum bandgap for decomposition of water is around 2.0 eV. On this basis alone, the most promising material would be α-Fe_2O_3 [23] with a band gap of 2.2 eV. The situation is similar for the wet photovoltaic cells. However, while a certain amount of overpotential is necessary to drive the reversible redox reaction on the electrode surface, the optimum band gap may be smaller since one has considerable freedom in choosing the redox couple.

If again the limitations of the electrochemical reaction kinetics are ignored, the semiconductor/electrolyte interface is very similar to a Schottky junction [24]. Several attempts have been made to apply this formalism to the semiconductor/electrolyte junction. The simplest picture is to follow the development of Gartner [24] and ignore any corrections to his model [16]. This seems to work quite well except near the flatband potential. In this model the electron–hole pair generation function is:

$$g(x) = \phi_0 \alpha \exp(-\alpha x), \qquad (3)$$

where ϕ_0 is the photon flux, α is the optical absorption coefficient and x the depth into the semiconductor (see Fig. 6).

The total photocurrent consists of two components: (1) from carriers generated in the depletion layer, and (2) from carriers generated in the bulk that diffuse into the depletion layer before recombining. The first component to the photocurrent is given by:

$$J_{dep} = e \int_0^W g(x)\,dx = -e\phi_0 [\exp(-\alpha W) - 1], \qquad (4)$$

where W is the width of the depletion layer and given by $W = W_0(V - V_{fb})^{1/2}$. W_0 is the depletion layer thickness for a potential of one volt across it. V_{fb} is the flatband potential measured relative to a reference electrode (usually the saturated calomel electrode, SCE) and V is the applied potential relative to the same reference electrode. W_0 depends on the doping density N_D and dielectric constant of the semiconductor ϵ in the following manner:

$$W_0 = (2\epsilon/eN_D)^{1/2}. \qquad (5)$$

The second component of the current is obtained by solving the diffusion equation for holes with suitable boundary conditions. The boundary conditions chosen are $p = p_0$ at $x = \infty$ and $p = 0$ at $x = W$, where p is the hole density and p_0 the equilibrium hole density. These particular boundary conditions are not good at $W \to 0$ or

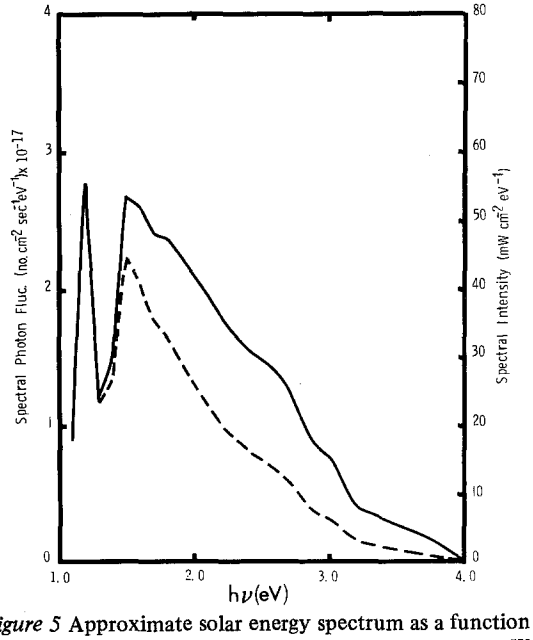

Figure 5 Approximate solar energy spectrum as a function of photon energy. The solid curve is solar flux in mW cm^{-2} eV^{-1} and the dashed curve is the number of photons cm^{-2} sec^{-1} eV^{-1} in units of 10^{17} for air mass one derived from data in [21]. At lower energies the dashed and solid curves are superimposed.

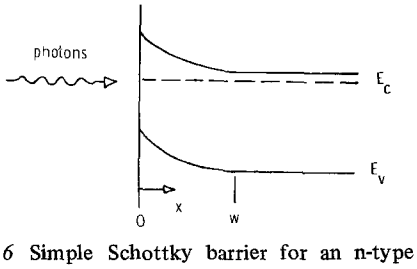

Figure 6 Simple Schottky barrier for an n-type semiconductor with a depletion layer formed at the junction. The conduction band E_c and the valence band E_v are shown together with the depletion layer thickness W.

near flatband conditions. The diffusion current is then given by:

$$J_{\text{diff}} = e\phi_0 \left[\frac{\alpha L_p}{1+\alpha L_p}\right] \exp(-\alpha W) \qquad (6)$$

where L_p is the hole diffusion length and we have neglected the term proportional to p_0 (the equilibrium hole density). This approximation is valid for large band gap semiconductors.

The total photocurrent is then given by:

$$J = e\phi_0 \left[1 - \frac{\exp[-\alpha W_0 (V - V_{fb})^{1/2}]}{1+\alpha L_p}\right]. \qquad (7)$$

This, then, describes the dependence of the photocurrent on the various parameters of the semiconductor ($\epsilon, N_D, \alpha, L_p, V_{fb}$). The dependence on photon energy enters through α and its dependence on photon energy. This model seems to work reasonably well as shown by the data for WO_3 in Fig. 7.

The limitations of the above model are that effects such as recombination at the interface are ignored and the boundary conditions are not adequate near flatband conditions. A number of models that correct for these deficiencies have been proposed. Kennedy and Frese have pointed out that near flatband the full Poisson–Boltzmann equation should be used to determine the potential [25]. This has allowed them to obtain a good fit to the potential behaviour of the photocurrent for some semiconductor/electrolyte interfaces near flatband conditions. Similarly, Wilson has included surface recombination in the Schottky model [26] and also obtains a good fit to the potential behaviour for some semiconductor/electrolyte interfaces near flatband conditions. Unfortunately, it is not clear in each case which of these factors is dominant, since not enough information is usually available from photocurrent measurements alone to distinguish the two cases. However, it is quite clear that both effects can be important.

Another approach to the problem is that of Laser and Bard [27]. By solving the equations which describe the behaviour of photoexcited carriers numerically, they have been able to include the electrochemical kinetics as well as surface recombination. The best approach depends strongly on the understanding of the particular semiconductor/electrolyte interface and knowing the dominant effects in the photoresponse.

All of the models discussed can be used to optimize the doping level for the semiconductor. Generally speaking, all photogenerated carriers should be useful in the photoelectrochemical processes. This means that $\alpha(W + L_p) \geqslant 1$ for all wavelengths. Close to the band gap energy α is small and consequently this requirement is more difficult to meet. This suggests that direct band gap materials in which α increases more rapidly for $h\nu > E_g$ would be more advantageous than indirect gap materials in which α increases less rapidly. For the metal oxide semiconductors and polycrystalline materials, the minority carrier diffusion length L_p is quite short. Then the condition for efficient utilization of photogenerated carriers becomes $\alpha W > 1$. Since the depletion layer thickness W depends on doping density N_D as shown in Equation 5, it is advantageous to use low doping levels consistent with a reasonable series resistance of the underlying bulk material. A possible way around these conflicting requirements is the use of non-uniform doping profiles. However, care must be taken to ensure that such profiles are stable and not subject to electromigration or diffusion of the donors [28]. It has been shown that substitutional donors

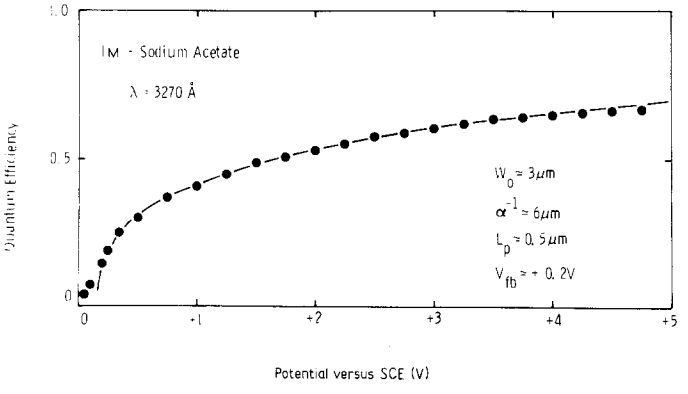

Figure 7 The quantum efficiency η of a WO_3 electrode as a function of applied potential for a monochromatic light source. The points are experimental data, while the line is a least squares fit to the data using the model of a simple Schottky barrier described in the text with three adjustable parameters (V_{fb}, α, L_p).

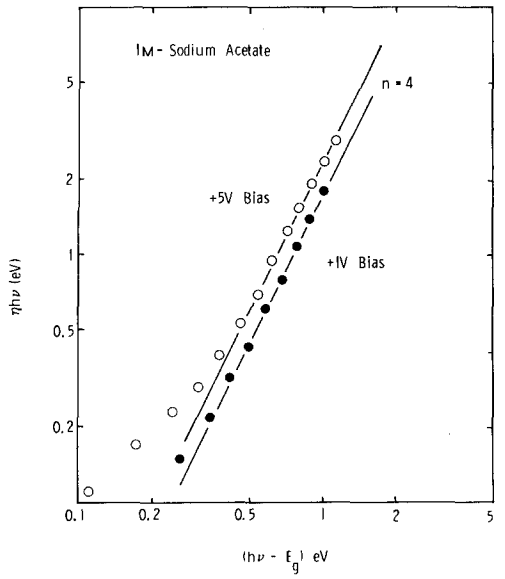

Figure 8 The behaviour of the quantum efficiency with photon energy as described in Equation 9 for WO_3. The solid lines correspond to $n = 4$ as expected for semiconductors with an indirect gap.

are more stable than defect dopants in metal oxide semiconductors [29].

It has been suggested that the dependence of photocurrent on wavelength may also be described by the Schottky model [16]. The

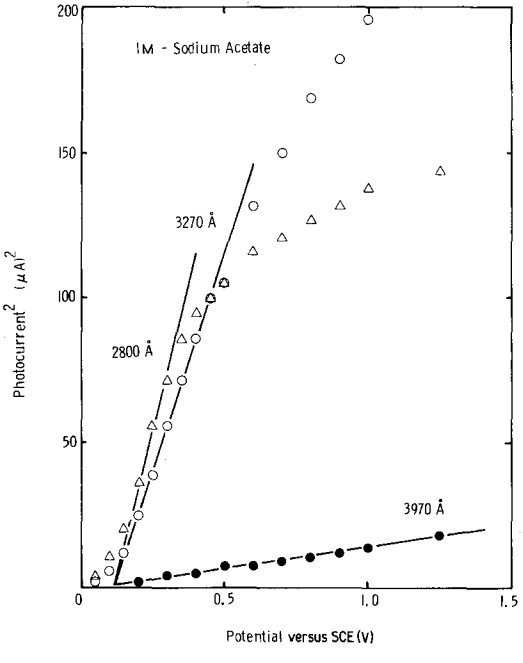

Figure 9 The square of the photocurrent versus applied potential for a WO_3 electrode at several wavelengths of incident light. The intercept is a measure of the flatband potential in this electrolyte.

optical absorption coefficient is assumed to have the following form above the band gap:

$$\alpha = A \frac{(h\nu - E_g)^{n/2}}{h\nu}, \tag{8}$$

where n is an integer and depends on whether the gap is direct ($n = 1$) or indirect ($n = 4$). Near the band edge, we would expect that $\alpha W \ll 1$ and the quantum efficiency $\eta \equiv J/e\phi_0$ may be written:

$$\eta \propto \alpha = A \frac{(h\nu - E_g)^{n/2}}{h\nu}. \tag{9}$$

While this expression seems to adequately describe the behaviour of WO_3 as shown in Fig. 8 and several other metal oxides, it has not been explored in detail for the non-oxides or semiconductors known to have a direct gap.

A number of important practical techniques for determining critical semiconductor parameters can be extracted from the Schottky barrier model. If $\alpha W_0 (V - V_{fb})^{1/2} \ll 1$ in Equation 7, then a plot of the square of the photocurrent versus applied potential will intercept the potential axis at the flatband potential, if there are not appreciable bulk recombination centres in the semiconductor. For increasing wavelength and thus decreasing α, the range of validity at this approximation increases correspondingly. The determination of V_{fb} for WO_3 by this method is illustrated in Fig. 9.

The conventional picture of solid-state devices and their efficiency is obtained from consideration of the current–voltage curve such as shown in Fig. 10. The power output of the device is just $P = IV$. At maximum output power the derivative of P

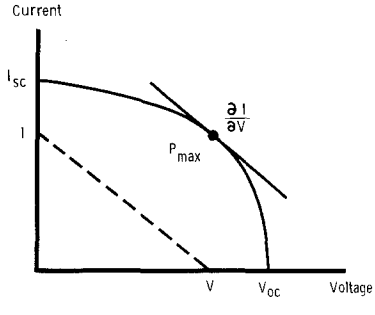

Figure 10 The current–voltage behaviour for a typical solid-state photovoltaic cell showing the short-circuit current I_{SC} the open-circuit voltage V_{OC} and the maximum output power point. At maximum power output $\partial I/\partial V$ the instantaneous slope (solid line) equals the average slope $-I/V$ (dashed line).

with respect to V should be zero, thus:

$$\frac{\partial P}{\partial V} = I + V\frac{\partial I}{\partial V} = 0, \qquad (10)$$

or, at P_{max}, we have:

$$\frac{\partial I}{\partial V} = -\frac{I}{V}. \qquad (11)$$

Another way of writing the maximum power output is $P_{max} = I_{SC}\, V_{OC} f$ where I_{SC} is the short-circuit current, V_{OC} the open circuit voltage and f the fill factor (how well the curve approximates a rectangle).

The description of a photovoltaic cell is also applicable to the photoelectrochemical variety and the maximum power point is determined in the same manner. The properties of the photoelectrochemical cell enter through V_{OC}, I_{SC} and f.

For PECs which have two redox couples and, therefore, produce a chemical product, the application of the model for solid state devices is somewhat complicated. The power produced is in terms of a chemical product and thus determined by current flow and the difference between the redox couples ($P_{out} = I\Delta V_{redox}$), if operated under short circuit conditions. However, most semiconductors cannot be used in this manner for splitting water since the electron affinity of the semiconductor is too large (see next section). Then an external bias must be applied to drive the cell. Power is then being put into the cell at the rate $P_{in} = IV_{bias}$. The net power produced is then:

$$P_{net} = I(\Delta V_{redox} - V_{bias}). \qquad (12)$$

This expression also allows for a cell which not only drives the chemical production process but may, in addition, produce electrical power by connecting a load between anode and cathode. In this case, the bias potential is negative. The description for photovoltaic cells can be applied to the chemical producing cells if we define an effective applied potential $V_{eff} = (\Delta V_{redox} - V_{bias})$. Then the description and determination of the maximum power point is the same as for photovoltaic cells.

The important point to make from this argument is that chemical producing cells should be biased to optimize their conversion efficiency, since only by accident would the semiconductor, electron affinity and redox potentials be correct for short-circuit conditions to correspond to the maximum power point. It is the efficiency of these biased cells that needs to be determined to know if a semiconducting electrode is useful in a chemical producing PEC.

3. Potential behaviour

The quantum efficiency of a PEC depends upon the material properties of the semiconductor and the electrolyte as well as other external factors such as temperature and external bias. In this section, additional factors are discussed which determine efficiency, with emphasis on the manner in which materials properties are important.

In the previous section we considered the nature of a number of factors in the semiconductor and how they affect efficiency, such as band gap and the nature of the gap (direct or indirect). The application of the Schottky model also illustrated the role played by doping level and minority carrier diffusion length. In this section the factors which determine open-circuit voltage for wet photovoltaic cells and the bias requirements for chemical producing photoelectrochemical cells are considered. Finally, the effects of temperature on photoelectrochemical cells will be considered.

From our previous discussion of the efficiency and maximum power operating point, it was evident that the short-circuit current and open-circuit voltage play an important role in determining the overall conversion efficiency. The short-circuit current is determined by the number of photons absorbed less the losses in the system. Thus, this depends primarily on factors we have already discussed. The open circuit voltage (or effective V_{OC} for chemical producing cells), however, depends on the relative positions of energy levels in both the semiconductor and the electrolyte (see Fig. 1).

The energy levels in the electrolyte (redox potentials) are generally known as a function of electrolyte composition [30] or can easily be determined. However, the energy levels in the semiconductor are more difficult to obtain. For semiconducting electrodes, the usual procedure is to measure some property which depends on applied potential and extrapolate to the flat-band condition.

The semiconductor/electrolyte interface can be represented as two capacitances in series; one in the electrolyte near the surface (Helmholtz

layer) C_H, and the other capacitor formed in the semiconductor by the depletion region C_{SC} [31]. Since these two capacitors are in series and $C_{SC} \ll C_H$, the net capacitance is $\sim C_{SC}$. The width of the depletion layer depends on the applied potential as illustrated in the previous section. Since the depletion layer width goes to zero at the flatband potential, the capacitance of the junction goes to infinity. The analysis of this type of behaviour for solid-state devices has shown that C^{-2} is linear in applied potential (Mott–Schottky plot). This approach can be applied to the semiconductor/electrolyte junction [4]. Typical data are illustrated for p-GaP in 0.1 M H_3PO_4 in Fig. 11. The flatband potential is the position of the Fermi level in the semiconductor when the depletion layer goes to zero width (no band bending) measured relative to whatever reference electrode is being employed.

With no depletion layer and, therefore, no electric field to separate the photogenerated electron–hole pair, the photocurrent should also go to zero at this potential. Differences between the onset of photocurrents and flatband potential determined from capacitance data indicates the existence of recombination centres or surface states in the semiconductor gap [32]. In many cases these are absent and the photocurrent onset can be used to determine the flatband potential.

Determination of the flatband potential is of crucial importance since it determines the maximum open-circuit voltage of a wet photovoltaic cell and the bias requirements of a chemical producing PEC. The potential difference between the semiconductor band edge and the redox potential at the counter electrode is the maximum obtainable band bending. A careful study of the factors affecting the flatband potential has shown that it may be expressed as [33]:

$$V_{fb} = EA - E_0 - \Delta_{fc} - \Delta_{px}, \qquad (13)$$

where EA is the semiconductor electron affinity measured from the vacuum level, E_0 is the reference electrode potential measured from the vacuum level, Δ_{fc} is the difference between the semiconductor fermi level and the conduction (valence) band for n-type (p-type) electrodes and Δ_{px} is the potential drop due to ions adsorbed on the semiconductor surface.

The problem then is to evaluate each of these factors so as to be able to predict V_{fb} for any semiconductor/electolyte combination. While

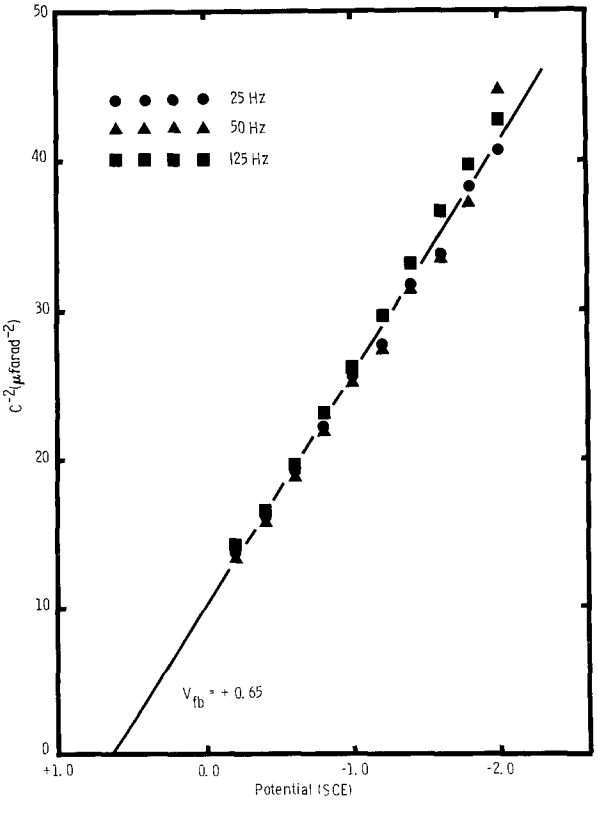

Figure 11 Mott–Schottky plot of the capacitance of p-GaP immersed in 0.1 M H_3PO_4 for several frequencies. The data are taken using a differential method.

there is some uncertainty, E_0 is taken to be 4.75 eV for the saturated calomel electrode (SCE) at 23° C [13]. Δ_{fc} can be evaluated from Seebeck coefficient measurements [34] and for the highly doped semiconductors commonly employed in PECs is typically 0.1 eV, a small correction. In the discussions which follow, this term will be ignored. The most important factors are EA and Δ_{px}.

A detailed understanding of adsorption of ions at the semiconductor/electrolyte interface is not possible at the present time. However, a number of things are known. If the flatband potential of the semiconductor shifts with concentration of ions in the electrolyte, then some species related to the ions in solution is specifically adsorbing on the semiconductor surface. For metal oxides in simple acids and bases, the flatband potential shifts by 59 mV/pH unit due to specific adsorption of H^+ and OH^-. These ideas have also been applied to non-oxides such as CdS [35]. The net surface charge depends on the relative electrochemical potentials for the two adsorbing species in the adsorbed state and in the solution. Since changing their concentration in the solution changes the electrochemical potentials, it is possible to vary the relative coverages of the two adsorbing species and thus the net surface charge [33]. Some concentration of ions in the solution exists at which the coverages by the two oppositely charged species are the same and thus the net surface charge is zero (point to zero zeta potential, PZZP). At this point, the potential drop due to adsorbed species is zero ($\Delta_{px} = 0$). Fortunately, techniques exist for determining this concentration of ions for any semiconductor/electrolyte combination [33, 35]. Thus, for metal oxides we may write:

$$\Delta\text{pH} = (59\text{ mV})(\text{pH}_{PZZP} - \text{pH}). \quad (14)$$

In general, it is possible to determine the PZZP of a semiconductor having only its undoped powder and thus it is not required to actually fabricate electrodes with all the ensuing difficulties.

The final factor we need to know in order to determine the flatband potential is the semiconductor electron affinity. This quantity is difficult to determine experimentally and impossible to calculate from first principles. However, considerable success has been achieved in calculating the electron affinity of several compounds using the atomic electronegativities of the constituent atoms [33, 35–37]. Mulliken defines the electronegativity of an atom as the arithmetic average of the energy to add and subtract a single electron. Thus, for neutral atoms, we have:

$$\chi_{atomic} = \tfrac{1}{2}(A + I_1), \quad (15)$$

where A is the atomic electron affinity and I_1 the first ionization potential. Both the electron affinity [38] and ionization potentials [39] are available for most atoms. For an intrinsic semiconducting solid, the corresponding energies are the bulk electron affinity EA and the energy at the valence band $EA + E_g$. Thus, in the bulk we have:

$$\chi_{bulk} = EA + \tfrac{1}{2}E_g. \quad (16)$$

The problem then is to relate the bulk electronegativity to the atomic electronegativities of the constituent atoms. Nethercot has postulated [36] that the bulk electronegativity is the geometric mean of the atomic electronegativities of the constituent atoms. This hypothesis seems to work for a large number of compounds. For example, for TiO_2 the electron affinity is:

$$EA(TiO_2) = \chi(TiO_2) - \tfrac{1}{2}E_g(TiO_2)$$
$$= [\chi(Ti)\,\chi^2(O)]^{1/3} - \tfrac{1}{2}E_g(TiO_2)$$
$$EA(TiO_2) = 4.33\text{ eV}. \quad (17)$$

With this method of determining the electron affinity it is now possible to predict the flatband

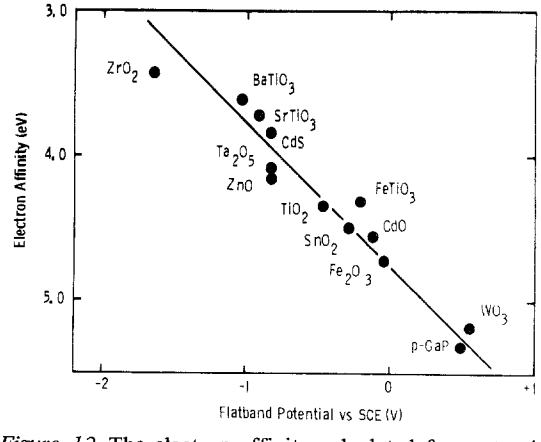

Figure 12 The electron affinity calculated from atomic electronegativities versus the measured flatband potentials of several semiconductors corrected to their respective PZZPs. The solid line is that expected from Equation 13 if Δ_{fc} is ignored. The data are from [32], [33] and [35]. The p-GaP data point refers to $EA + E_g$ rather than the electron affinity.

potential for any semiconductor/electrolyte combination. Correcting all measurements to the PZZP allows a direct comparison of the calculated electron affinities with the measured flatband potentials. Fig. 12, shows such a comparison for a number of different semiconductors and the agreement is clearly quite good.

Thus, the electronegativity model combined with an understanding of the effects of specific ion adsorption allows a prediction of the flatband potential for any semiconductor/electrolyte interface. This knowledge and the knowledge of the energy level structure in the electrolyte enables us to predict the maximum open-circuit voltage for a wet photovoltaic cell or the bias requirements for a chemical producing cell.

Another important aspect of the electronegativity model is that it provides an understanding of the role atomic properties play in determining the behaviour of a semiconducting electrode. For semiconducting anodes an important requirement is as small an electron affinity as possible [40] to maximize the open-circuit voltage or minimize the applied bias. Since oxygen is a very electronegative atom, the model suggests that metal oxides with small oxygen content would be the most useful in this respect.

Another quantity which appears to correlate with electron affinity for metal oxides is band gap. The argument has been made that since the valence band is formed by O(2p) levels, which will be approximately the same for all oxides, decreasing electron affinity corresponds to increasing band gap and vice versa [41]. Both of these arguments are illustrated in Fig. 13. It is apparent that there is indeed a correlation between band gap and electron affinity, if the data are restricted to compounds with about the same atomic per cent oxygen. The figure suggests that compounds with small metal valences and therefore low oxygen content such as Cu_2O would be the most fruitful to explore. However, there is some question as to the stability of this class of compounds. The atomic electronegativity model has been used to explain the difference between Fe_2O_3 and $YFeO_3$ where the electron affinity is lowered by replacing Fe by Y [42].

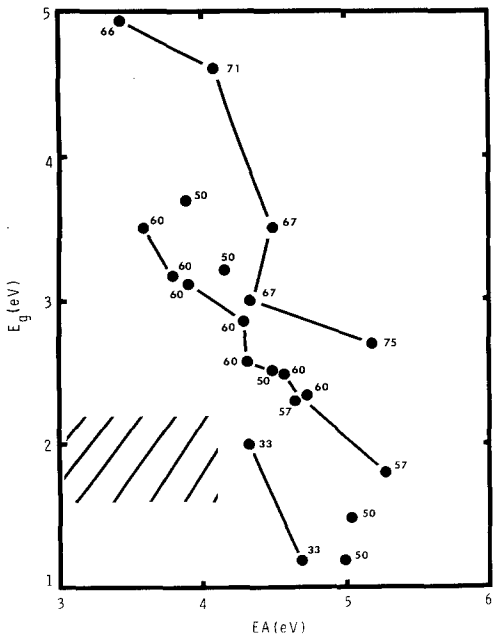

Figure 13 Measured bandgap versus the electron affinity calculated using the atomic electronegativity model. The numbers are the at.% oxygen. The cross-hatched area is the optimum region for photoelectrolysis.

Another external factor affecting cell efficiency is temperature. This could be quite important for the application of photoelectrochemical cells in concentrator systems where the cells would operate at elevated temperatures. The basic mechanism for temperature-dependent effects is shifts in the energy levels of both the semiconductor and electrolyte with temperature and changes in the electrochemical reaction rates. Shifts in energy level positions can cause two effects: changes in band gap and thus optical response and changes in bias requirements for chemical producing cells or open-circuit voltage for photovoltaic cells. There is also some effect of elevated temperature on degradation mechanisms such as donor migration. All of these factors have not been explored.

Changes of optical response in SnO_2 with increasing temperature have been observed and attributed to thermally induced band gap changes [43]. Generally speaking, these effects are quite small and result in decreasing band gaps with increasing temperature. This is, of course, a beneficial effect.

The potential shifts with temperature are somewhat more complex [44]. Both the potentials in the electrolyte and semiconductor will shift with temperature. These can be sorted out by considering Equation 13. All of the factors in this expression will be temperature dependent. The temperature dependence of E_0 is due to the temperature dependence of the reference electrode. The Fermi level in the semiconductor also

shifts with temperature and thus changes Δ_{fc}. This may be estimated from Seebeck measurements as a function of temperature. Finally, the potential drop due to adsorbed ions will be temperature dependent. This arises from two effects: the electrochemical potential of ions in solution is temperature dependent as well as the electrochemical potential of the adsorbed ions. Fortunately, these effects can be measured [44].

These are the factors then which determine the temperature dependence of the flatband potential. Measurements for TiO_2 indicate that these effects are small $\lesssim 0.1$ V between 0 and 100° C in aqueous electrolyte and that these results are typical for all metal oxides [44]. The bias requirements for a chemical producing cell or open-circuit voltage for a photovoltaic cell depend on the difference between the flatband potential and the relevant redox potential. Thus, the temperature dependence of the couple must also be included.

We have considered the effect of the semiconductor energy level positions on the potential requirements for the cell. In the case of the photoelectrolysis cell, where the redox couples are essentially fixed by the desired reaction products, this will be the primary concern because there is little flexibility in choosing the constituents of the electrolyte. In the wet photovoltaic cells, however, barring the constraints imposed by the stability of the electrode which will be discussed in the next section, considerable flexibility exists in the choice of the reversible redox couple to be employed.

These factors and this information will then allow predictions of changes in bias requirements or open-circuit voltages for any PEC and their dependence on temperature.

4. Stability

As has been previously mentioned, one of the three key criteria for the practical photoelectrode is its stability. The electrode must be stable to dissolution, photocorrosion and electrochemical corrosion. A number of different types of instabilities that are commonly encountered in photoelectrolysis and wet photovoltaic cells can be distinguished. The nature and ramifications of some of these instabilities for each type of cell will now be discussed, roughly in order of importance.

By far the dominant concern in any assessment of electrode stability must be the intrinsic thermodynamic stability of the electrode. Gerischer [14] and Bard and Wrighton [15] have recently discussed simple models of the thermodynamic stability of a photoelectrode.

The main concern is whether the reaction of interest is thermodynamically more or less favourable than the appropriate oxidative or reductive decomposition reactions for the semiconductor. The completely stable case occurs when the reductive decomposition reaction potential lies above (more negative than) the conduction band and the oxidative decomposition potential lies below (more positive than) the valence band edge (Fig. 14). Under these conditions, the electrode cannot provide electrons or holes with sufficient energy to drive the decomposition reactions. No example of this case has yet been found. Various semiconductor/electrolyte combinations appear more like b, c and d in Fig. 14. Here the electrode is respectively unstable, stable against cathodic decomposition and stable against anodic decomposition.

The situation would appear discouraging from this aspect alone; however, attention must be directed toward the relative positions of the decomposition potentials and the redox potential of interest. Fig. 15 illustrates typical examples for a photoelectrolysis cell and for a wet photovoltaic cell. In the photoelectrolysis case, if the decomposition potential lies above the reaction potential as in (a), then the potential drop for

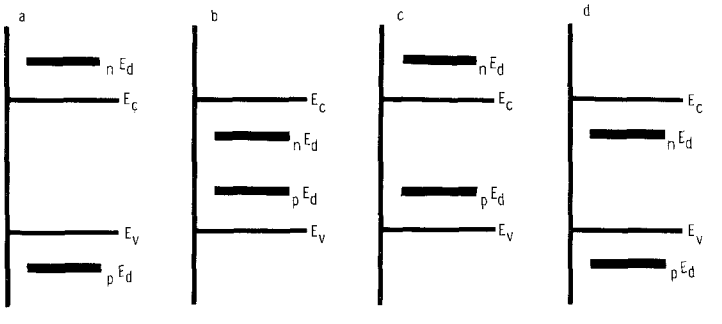

Figure 14 The relative positions of semiconducting electrode conduction E_c and valence E_v band edges and decomposition potentials for anodic $_pE_d$ cathodic $_nE_d$ decompositions (a) Stable against both anodic and cathodic decomposition, (b) unstable against both anodic and cathodic decomposition, (c) stable against cathodic and unstable against anodic decomposition, (d) unstable against cathodic and stable against anodic decomposition.

an electron going to the hole at the valence band edge is greater for the decomposition reaction than for the oxygen evolution reaction. This potential drop or "effective overpotential" [16] is a measure of the relative driving force available for the two reactions. This is the case appropriate to ZnO [45] and here decomposition competes successfully with oxygen production. In case (b), the overpotential available for oxygen production is greater than that for the decompositon reaction and one would expect preferential O_2 production. This case is typical of TiO_2 photoanodes and, in fact, these electrodes are among the most robust of any known. Thus, it is the relative positions of the decomposition potential and the desired redox couple that determines stability rather than the valence band position. This illustrates the role that kinetics, as influenced by the effective overpotential, can play in determining whether the electrode will decompose or perform the desired electrochemistry.

CdS [46] is like ZnO thermodynamically and has been found to be unstable as have all non-oxides tried thus far for photoelectrolysis. This brings up one of the major problems facing photoelectrolysis cells. In general, the oxides are the most thermodynamically stable compounds and oxygen is available in nearly atomic form on the surface of a photoanode. Thus, it is highly likely that any non-oxide will grow an interfering oxide layer. So far this has always been found to occur. Therefore, one must strive to find a stable oxide for the photoanode with the decomposition potential below the O_2/OH^- level and which satisfies other requirements for efficient operation.

A convenient method for exploring the stability range of various electrode materials has recently been demonstrated by Park [47]. Pourbaix diagrams can be calculated which show the thermodynamic stability of various semiconductor materials over a wide range of electrolyte composition. This approach, while not considering the reaction kinetics and surface ion effects, does serve as a fundamental guide to electrode stability as a function of electrolyte composition and what might be the decomposition pathways. Fig. 16 is a typical Pourbaix diagram for CdS.

The second major problem in photoelectrolysis or any photoelectrochemical cell producing chemical products is the limited flexibility to modify the stability of the system. For a given oxide photoanode, the conduction and valence band edges of the semiconductor are fixed by the semiconductor's electron affinity and band gap. The positions of the redox reactions are necessarily fixed by the specific chemistry desired. Thus, if the decomposition potentials fall propitiously in the right places, the electrodes may be stable; however, if they do not, very little

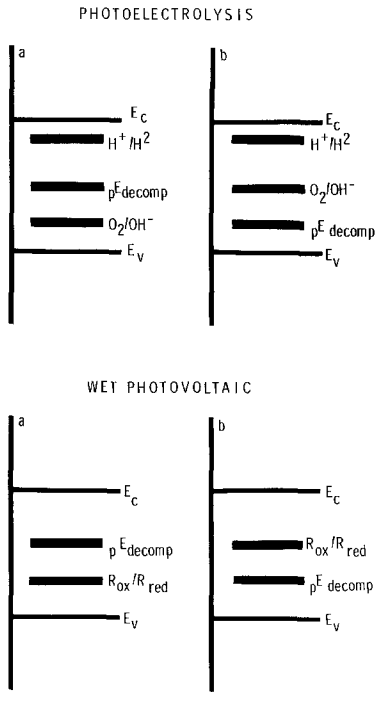

Figure 15 Relative positions of decomposition potentials and desired redox potentials for photoelectrolysis and wet photovoltaic cells using n-type semiconducting electrodes. All examples are thermodynamically unstable, but (b) is kinetically more stable than (a). See text for details.

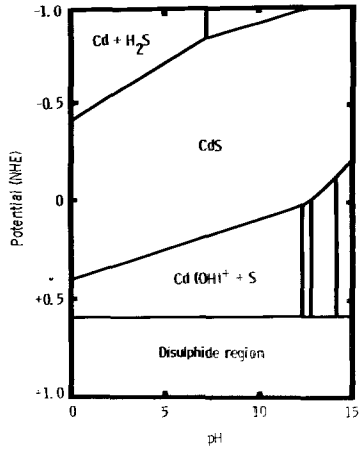

Figure 16 Pourbaix diagram for CdS in an aqueous electrolyte. The predominant species in the various regions of potential and pH are indicated.

TABLE I Decomposition in reaction potentials for CdS in aqueous electrolyte

Reaction	Electrolyte	E_d (NHE)
$CdS = Cd^{2+}_{aq} + S + 2e^-$	1 M KCl	0.32
$CdS + S^{2-}_{aq} = Cd^{2+}_{aq} + S^{2-}_{2aq} + 2e^-$	1 M S^{2-}/S^{2-}	−0.48
$CdSe = Cd^{2+}_{aq} + Se + 2e^-$	1 M KCl	0.12
$CdSe + S^{2-}_{aq} = Cd^{2+}_{aq} + Se + S^{2-}_{aq} + 2e^-$	1 M S^{2-}/S^{2-}_2	−0.45
$S^{2-}_{2aq} + 2e^- = 2S^{2-}_{aq}$	1 M NaOH	−0.48

can be done (with the exception of surface modification) to improve the stability.

The situation is considerably more flexible in the case of wet photovoltaic cells. As the lower portion of Fig. 15 illustrates, the same basic thermodynamic constraints exist here as in the photoelectrolysis cells. If the decomposition potential lies above the reversible redox couple, the electrode will be thermodynamically unstable. If the reverse is true, it may be stable if the kinetics are favourable. Since all that is required is a reversible couple with the appropriate energetics and kinetics, one may tailor a couple to the semiconductor and achieve a relatively high degree of stability. This has been done for a large number of cells typified by the n-CdS/S^{2-}, NaOH, S/Pt cell [48] and the n-$GaAs/Se^{2-}$, Se^{2-}_2, KOH/C cell [49]. The application of this concept is well illustrated by the n-$CdTe/Te^{2-}$, $Te^{2-}_2OH^-$/Pt cell [50]. As the band gap is reduced from that of CdS (2.4 eV) to that of CdTe (1.4 eV), the electrode is no longer stable in an S^{2-}/S^- electrolyte and one must go to a Te^{2-}/Te^{2-}_2 electrolyte. This ability to use different couples in the cell provides a larger degree of freedom with respect to optimizing cell stability. However, care must be taken to see that such changes do not reduce the open-circuit voltage of the cell which is a function of the separation between the conduction band edge and the redox potential.

While the basic thermodynamic and kinetic stability of the electrode is, of course, the primary concern, a number of other mechanisms which degrade cell open-circuit potential and quantum efficiency have been identified. For wet photovoltaic cells, a fundamental concern is the rigorous exclusion of oxygen from the system to avoid oxide formation at the electrode surface [48, 49]. In addition, many of the electrolytes are unstable with respect to oxidation and large oxide anions can result in degraded cell performance, particularly in the case of S^{2-}, Se^{2-} and Te^{2-}. Another stability problem affecting the electrolyte is long-term degradation from precipitation of insoluble polyions.

It has recently been demonstrated [51, 52] that in the $CdSe/S^{2-}$, S^-, NaOH/C cell, one can get ion exchange of the surface layer which results in the formation of a CdS surface layer on the CdSe electrode. Since the valence band edge of CdS is about 0.5 eV below that of CdSe, this produces a 0.5 eV barrier which results in a drop in photocurrent. This sort of problem can be avoided by having common anions in the electrode and the electrolyte or by having a situation where the anion in the electrolyte cannot grow an epitaxial layer on the electrode. This process can really be thought of as another form of decomposition whereby the energy required for substitution E(Se/S) lies appropriately above E (redox) (Table I summarizes the appropriate E_ds). An indication of this is that the reaction $CdSe + S^{2-} \rightarrow CdS + Se^{2-}$ seems to occur to some extent in the dark at slightly anodic potentials or even as a pure corrosion process. Thus, the thermodynamics of substitution must be examined, as well as decomposition, for both electrode and electrolyte. These results indicate that polychalcogenide electrolytes may not be the panacea originally hoped for.

Gerischer and Gobrecht have recently shown [52] that long-term ageing of CdS and CdSe photoanodes can cause phase changes in the surface layer. A transformation of the surface of CdSe or CdS single crystal photoanodes under illumination in sulphide/polysulphide redox electrolytes to polycrystalline or amorphous phases was observed. Concurrent with the phase changes were significant reductions in the photocurrents. This problem may well be significant in many of the non-oxide electrodes.

Considerable attention has been directed recently at the importance of surface states and surface ageing in a number of the transition metal oxide anodes employed in photoelectrolysis cells. Wilson and Harris [43, 54] have shown that surface reaction intermediates are important for the oxygen evolution on TiO_2 and that there is slow surface erosion on TiO_2 perhaps through some of the long half-life intermediates. Butler

[28] has shown that for defect-doped TiO_2 electromigration of Ti^{3+} interstitials out of a TiO_2 photoanode occurs under mild anodic bias. This reduction of the doping level near the surface changes the depletion layer width and can result in decreases in the photocurrent. Ginley and Knotek [55] have demonstrated that hydrogen in the TiO_2 surface layer plays a crucial role not only as a reaction intermediate but in determining the electrical properties of the electrode as well. Cathodic ageing of TiO_2 or $SrTiO_3$ anodes in 1 M NaOH introduced hydrogen into a thin surface layer drastically changing both photoresponse and flatband potentials. These effects are illustrated for a TiO_2 electrode in Fig. 17. These problems regarding the nature of the dopants and the importance of chemisorbed species have just begun to be addressed and may prove crucial.

A number of approaches have been employed to circumvent or limit decomposition. Most of the wet photovoltaic cells can be stabilized to a large extent by the appropriate choice of a redox couple. If they cannot be stabilized, considerations are much the same as for photoelectrolysis cells. We will therefore concentrate on techniques to improve the stability of photoanodes for photoelectrolysis. The instability of the electrode surface of some oxides and of non-oxides has resulted in a number of attempts to introduce charge transfer intermediates on the electrode surface. If the kinetics of the charge transfer are fast enough, the electrode might be stabilized. Earliest among these were the attempts of Gerischer [56] to employ dye sensitization. Here organic dyes were chemisorbed on oxide surfaces, typically rhodamines on ZnO. The energy level diagram for such a system is illustrated in Fig. 3. Upon light absorption, the dye injects an electron into the semiconductor, the remaining hole reacts spontaneously with the electrolyte. This approach is generally successful within the limits of the inherent stability of the dye, but due to the low optical density of thin dye layers, only very small net conversion efficiencies were obtained. Wrighton *et al.* [57, 58] have taken the reverse approach. By chemically bonding an efficient charge transfer agent, ferrocene as 1-trichlorosilyl ferrocene and as 1–1′ dichlorosilyl ferrocene, to the surface of Si and Ge they have observed charge transfer through the ferrocene linkage from semiconductor to electrolyte as the major current pathway. Here a major advantage is that light absorption occurs in the semiconductor and not the attached charge transfer intermediate, thus higher collection efficiencies should be obtained.

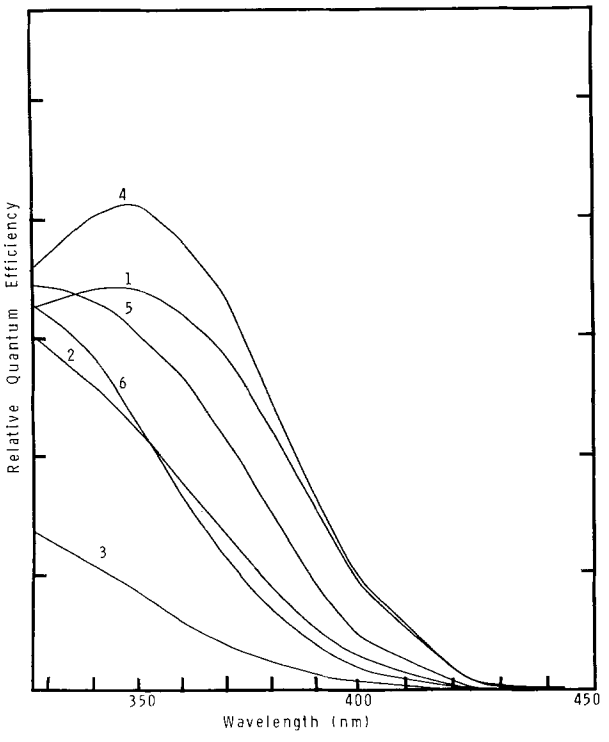

Figure 17 The relative quantum efficiency as a function of wavelength for a lightly hydrogen-reduced TiO_2 sample successively aged in 1 M NaOH. The changes in photoresponse result from electroinjection and migration of H^+ and electromigration of Ti^{3+} interstitials. (1) Virgin sample, (2) 100 μA, 14 h cathodic, (3) 100 μA, 20 h cathodic, (4) 0.0 V(SCE) 20 h, (5) + 1.0 V(SCE) 23 h, and (6) + 5.0 V(SCE) 4 days.

Although conversion efficiencies are low, enhanced electrode stability does result and hope for more efficient permanently attached intermediates remains. In an elegant experiment [59] McGregor *et al.* have shown that an *in situ* synthesized Zn-phthalocyanine layer on a ZnO photoanode stabilizes it significantly against photodissolution and at the same time does not greatly limit the photocurrents produced. The idea of chemically bonding or chemisorbing complexes with very small solubility products and high photostabilities on oxides and non-oxides appears to have applicability to electrochemistry in general.

Another approach is to overcoat the surface of an unstable, small band gap semiconductor with a thin layer of a more stable higher band gap oxide semiconductor. This concept was first discussed by Wagner and Shay [60] and later by Nozik [61]. This approach offers the potential for greater stability and if the electron affinities of the materials are appropriate, such that *EA* of the small band gap semiconductor is smaller than *EA* for the larger band gap semiconductor, then larger open-circuit potentials result. Nozik [61] has shown for n-TiO_2 on n-GaAs and n-SnO_2 on n-Si that enhanced stabilities and larger open-circuit potentials do result; however, photocurrents are reduced.

Improved stability has also been obtained by the introduction of charge-transfer solution species to the electrolyte to act as reaction intermediates. Harris *et al.* [62] have shown that by adding cobaltous ions to the electrolyte in a TiO_2/NaOH/Pt cell, all corrosion was suppressed. Here the Co^{2+} ion acts as a rapid electron transfer agent effectively competing with corrosion.

Another approach used by the groups of Bard [63] and Schwerzel [64] has been to change the anode electrochemistry. The main goal of the photoelectrolysis cell is hydrogen production. Thus, if an alternate anode chemistry could be found that used cheap materials and produced a useful product while stabilizing the anode, it might prove a viable alternative. They have shown that the Kolbe electrolysis, turning carboxylic acids into hydrocarbons and CO_2 will run efficiently at various oxide photoanodes. In fact, because of the mechanism of current doubling, where a second electron from the electron transfer intermediates is injected directly into the conduction band, enhanced photocurrents are observed.

Tributsch [38, 39, 65] has recently shown that photoanodes made of MoS_2, $MoSe_2$, WS_2, etc., have a high stability and reasonable conversion efficiency in basic electrolytes. This is interesting because in these materials the photon excites a d–d transition on the metal ions rather than the anion to cation charge transfer transition typical of most other semiconducting materials. This means that the photoexcitation does not produce large changes in bonding electron density which perhaps stabilizes these materials.

Finally, Parkinson *et al.* [66] have shown that the treatment of an n-GaAs photoanode in an n-GaAs/Se^{2-}, Se_2^{2-}, OH^-/C cell with ruthenium ions greatly enhances cell efficiency. One possible explanation for this effect is that the Ru ions act as charge transfer intermediates while removing a trap that otherwise would limit the production of useful photocurrents. Thus, such treatments would remove both electron hole traps and defects causing decomposition.

It is apparent that the stability of photoelectrochemical cells is a complex subject. A number of guidelines now exist for addressing the thermodynamic stability of various semiconductor/electrolyte combinations. The importance of electromigration and chemisorption of ions in and on semiconductor surfaces has been recognized. If unstable electrodes are to be used, they must be overcoated with stable materials or a passivating charge-transfer intermediate must be employed.

5. Future directions

From the foregoing discussion, it is clear that significant progress has been made in recent years in understanding the factors which are important in determining the efficiency of photoelectrochemical cells. The similarity between these devices and solid-state devices has allowed the modelling of the semiconductor optical response. This, in turn, has determined a number of the important materials properties of the semiconducting electrodes, such as band gap, electron affinity, doping level, etc. Two additional factors complicate the behaviour of PECs over solid state [55] devices. The stability of these cells is significantly more complex than for solid-state devices. While some progress has been made in understanding the thermodynamic aspects of stability, it seems that kinetics will be the determining factor for future applications of PEC devices.

Practical devices require stability in terms of many years rather than weeks that have been demonstrated in the laboratory to date. Stability then will probably be *the* important area of research in the future. The second difference between PEC devices and SS devices is the charge transfer process across the semiconductor/electrolyte interface. At the present time little is understood about the details of this process. One important question is the role played by surface states. Unfortunately, little is known about solid–liquid interfaces in general compared with solid–vacuum interface where many surface science techniques may be applied, the major constraint being the lack of experimental techniques which allow one to directly probe the electronic structure of the solid–liquid interface. It is likely that in the future this area of research will develop and ultimately contribute to our knowledge of the fundamentals of charge transfer at the semiconductor/electrolyte interface.

At the present time our basic knowledge is neither sufficient to allow the ultimate electrode material to be identified nor to definitely answer the question of practicality for PEC devices. Only the direction in which the field is developing can be seen and opinions hazarded about what may be expected in the future. It is generally accepted that any solar energy conversion devices must be at least 10% efficient to be of any practical value. At the present time, PEC devices which generate electricity have already surpassed this goal [66]. The remaining questions involve stability and the economic and environmental aspects of the materials involved. For chemical producing PECs limited progress has been made with respect to efficiency but a much greater range of possibilities remain to be explored. Essentially all of the work in this area has involved the decomposition of water into H_2 and O_2. Currently, the most efficient cell (probably Fe_2O_3 or TiO_2 with an external bias) is at best a few per cent efficient. The difficulties arise from the large electrochemical potential necessary for the decomposition of water. This has created stability problems for all semiconducting photoanodes except oxides. As discussed previously, the correlations between flatband and band gap for the oxides has limited the efficiency available from these materials. It is possible that some progress can be made by using both photoanodes and photocathodes to decrease bias requirements. However, at the present time it appears that efficiencies greater than 10% will be exceedingly difficult to obtain when decomposing water.

Some of these problems may be alleviated by considering an area that has been neglected up to now. PECs may be used to drive reactions other than the decomposition of water. By proper choice of reaction, stability may be improved while still producing a useful fuel. This area of research offers many fascinating possibilities.

Acknowledgement

This work was supported by the Materials Sciences Program, Division of Basic Energy Sciences, US Department of Energy, under Contract DE-AC04-76-DP00789.

References

1. E. BECQUEREL, *Compt. Rend. Acad. Sci. Paris* **9** (1839) 561.
2. W. H. BRATTAIN and C. G. B. GARRETT, *Bell System Tech. J.* **34** (1955) 129.
3. H. GERISCHER, in "Advances in Electrochemistry and Electrochemical Engineering", edited by P. Delahay (Interscience, New York, 1961) p. 139.
4. *Idem*, in "Physical Chemistry: An Advanced Treatise", Vol. 9A, edited by H. Eyring, D. Henderson and W. Jost (Academic Press, New York, 1970).
5. A. FUJISHIMA, K. HONDA and S. KIKUCHI, *J. Chem. Soc. Japan* **72** (1969) 108.
6. A. FUJISHIMA and K. HONDA, *Nature* **238** (1972) 37; *Bull. Chem. Soc. Japan* **44**, (1971) 1148; *J. Chem. Soc. Japan* 74 (1971) 355.
7. M. D. ARCHER, *J. Appl. Electrochem.* **5** (1975) 17.
8. W. A. GERRARD and L. M. ROUSE, *J. Vac. Sci. Technol.* **15** (1978) 1155.
9. J. MANASSEN, D. CAHEN and G. HODES, *Nature* **263** (1976) 97.
10. A. J. NOZIK, *Ann. Rev. Phys. Chem.* **29** (1978) 189.
11. A. J. BARD, American Ceramic Society Fall Meeting, Dallas, Texas, 19 September (1978).
12. A. J. NOZIK, 2nd International Conference on Photochemical Conversion and Storage of Solar Energy Cambridge, England, 10 August (1978).
13. F. LOHMANN, *Z. Naturforsch. A.* **22** (1967) 843.
14. H. GERISCHER, *J. Electroanal. Chem.* **82** (1977) 133.
15. A. J. BARD and M. S. WRIGHTON, *J. Electrochem. Soc.* **124** (1977) 1706.
16. M. A. BUTLER, *J. Appl. Phys.* **48** (1977) 1914.
17. A. B. BOCARSLY, J. M. BOLTS, P. G. CUMMINS and M. S. WRIGHTON, *Appl. Phys. Letters* **31** (1977) 568.
18. J. O. M. BOCKRIS and A. K. N. REDDY, "Modern Electrochemistry", Vol. 2 (Plenum, New York, 1970) p. 862.
19. J. HOARE, "The Electrochemistry of Oxygen" (Wiley, New York, 1968) p. 82.

20. R. E. SCHWERZEL, E. W. BROOMAN, R. A. CRAIG and V. E. WOOD, in "Semiconductor Liquid-Junction Solar Cells", edited by A. Heller (Electrochemical Society, Princeton, 1977) p. 293.
21. M. T. THEKAEKARA, Survey of Quantitative Data on Solar Energy and Its Spectral Distribution, in Proceedings of Conference Compiles (Cooperation Mediterranienne Sur l'Energie Solaire) Dahran, Saudi Arabia (November 1975).
22. H. J. HOVEL, "Semiconductors and Semimetals", Vol. II (Academic, New York, 1975).
23. R. K. QUINN, R. D. NASBY and R. J. BAUGHMAN, *Mat. Res. Bull.* **11** (1976) 1011.
24. W. W. GARTNER, *Phys. Rev.* **116** (1959) 84.
25. J. H. KENNEDY and K. W. FRESE, *J. Electrochem. Soc.* **125** (1978) 709.
26. R. H. WILSON, *J. Appl. Phys.* **48** (1977) 4292.
27. D. LASER and A. J. BARD, *J. Electrochem. Soc.* **123** (1976) 1828, 1833, 1837.
28. M. A. BUTLER, *J. Electrochem. Soc.* **126** (1979) 338.
29. C. E. DERRINGTON, W. S. GODEK, C. A. CASTRO and A. WOLD, *Inorg. Chem.* 17 (1978) 977.
30. D. DOBOS, "Electrochemical Data" (Elsevier, New York, 1975).
31. A. K. VIJH, "Electrochemistry of Metals and Semiconductors" (Dekker, New York, 1973).
32. D. S. GINLEY and M. A. BUTLER, Electrochemical Society Meeting, Boston, Mass. 5–6 November (1979).
33. M. A. BUTLER and D. S. GINLEY, *J. Electrochem. Soc.* **125** (1978) 228.
34. N. B. HANNAY, "Semiconductors" (Reinhold, New York, 1959).
35. D. S. GINLEY and M. A. BUTLER, *J. Electrochem. Soc.* **125** (1978) 1968.
36. A. H. NETHERCOT, *Phys. Rev. Letters* **33** (1974) 1088.
37. R. T. POOLE, D. R. WILLIAMS, J. D. RILEY, J. G. JENKINS, J. LIESEGANG and R. C. G. LECKEY, *Chem. Phys. Letters* **36** (1975) 401.
38. H. HOTOP and W. C. LINEBERGER, *J. Phys. Chem. Ref. Data* **4** (1975) 539.
39. F. A. WHITE, "Mass Spectrometry in Science and Technology" (Wiley, New York, 1968).
40. J. G. MAVRIODES, D. I. TCHERNEV, J. A. KAFALAS and D. F. KOLESAR, *Mat. Res. Bull.* **10** (1976) 1023.
41. H. H. KUNG, H. S. JARRETT, A. W. SLEIGHT and A. FERRETTI, *J. Appl. Phys.* **48** (1977) 2463.
42. M. A. BUTLER, D. S. GINLEY and M. EIBSCHUTZ, *ibid* **48** (1977) 3070.
43. M. S. WRIGHTON, D. L. MORSE, A. B. ELLIS, D. S. GINLEY and H. B. ABRAHAMSON, *J. Amer. Chem. Soc.* 98 (1976) 44.
44. M. A. BUTLER and D. S. GINLEY, *Nature* **273** (1978) 524.
45. B. PETTINGER, R. SCHOEPPEL and H. GERISCHER, *Ber. Bunsenges Phys. Chem.* 78 (1974) 1024.
46. H. GERISCHER and J. GOBRECHT, *ibid* **80** (1976) 327.
47. S. M. PARK and M. E. BARBER, *J. Electroanal. Chem.* **99** (1979) 67.
48. A. B. ELLIS, S. W. KAISER and M. W. WRIGHTON, *J. Amer. Chem. Soc.* 98 (1976) 1635.
49. K. C. CHANG, A. HELLER, B. SCHWARTZ, S. MENEZES and B. MILLER, *Science* **196** (1977) 1097.
50. A. B. ELLIS, S. W. KAISER and M. W. WRIGHTON, *J. Amer. Chem. Soc.* 99 (1977) 2839.
51. A. HELLER, A. P. SCHWARTZ, R. G. VADIMSKY, S. MENEZES and B. MILLER, *J. Electrochem. Soc.* **125** (1978) 1156.
52. H. GERISCHER and J. GOBRECHT, *Ber. Bunsenges Phys. Chem.* **82** (1978) 520.
53. L. A. HARRIS and R. H. WILSON, *J. Electrochem. Soc.* **123** (1976) 1010.
54. R. H. WILSON, Electrochemical Society Meeting, Extended Abstracts Vol. 78-1 (Seattle, WA, 1978) p. 415.
55. D. S. GINLEY and M. L. KNOTEK, *J. Electrochem. Soc.* (in press).
56. H. GERISCHER and H. TRIBUTSCH, *Ber. Bunsenges Phys. Chem.* **72** (1968) 437; *ibid.* 73 (1968) 251.
57. M. S. WRIGHTON, J. M. BOLTS, A. B. BOCARSLY, M. C. PALAZZOTTO and E. G. WALTON, *J. Vac. Sci. Tech.* **15** (1978) 1429.
58. J. M. BOLTS and M. S. WRIGHTON, *J. Amer. Chem. Soc.* **100** (1978) 5257.
59. K. G. McGREGOR, J. W. OTVOS and M. CALVIN, 2nd International Conference on Photochemical Conversion and Storage of Solar Energy, Cambridge, England (1978).
60. S. WAGNER and J. SHAY, *Appl. Phys. Lett.* **31** (1977) 446.
61. A. J. NOZIK, 2nd International Conference on Photochemical Conversion and Storage of Solar Energy, 8/10-12/78, Cambridge, England.
62. L. A. HARRIS, D. R. CROSS and M. E. GERSTNER, *J. Electrochem. Soc.* **124** (1977) 839.
63. B. KRAEULTER and A. J. BARD, *J. Amer. Chem. Soc.* **100** (1978) 2239, 5985.
64. R. E. SCHWERZEL, E. W. BROOMAN, R. A. CRAIG, F. R. MOORE, L. E. VAALER and V. E. WOOD, Electrochemical Society Meeting Extended Abstracts Vol. 78-1, No. 413, Seattle, Washington May 21 (1978).
65. H. TRIBUTSCH, *J. Electrochem. Soc.* **125** (1968) 1086.
66. B. A. PARKINSON, A. HELLER and B. MILLER, *Appl. Phys. Letters* **33** (1978) 521.

Received 3 April and accepted 6 June 1969.